THE AMERICAN SOCIETY OF MECHANICAL ENGINEERS
345 E. 47th St., New York, N.Y. 10017

95-GT-198

OGV Tailoring to Alleviate Pylon-OGV-Fan Interaction

G. N. Shrinivas* M. B. Giles†
Oxford University Computing Laboratory, Oxford, U.K.

Abstract

This paper studies the application of sensitivity analysis to the redesign of outlet guide vanes (OGV's) in a commercial gas turbine engine. The redesign is necessitated by the interaction of the pylon induced static pressure field with the OGV's and the fan, leading to reduced OGV efficiency and shortened fan life. The concept of cyclically varying camber is used to redesign the OGV row to achieve suppression of the downstream disturbance in the domain upstream of the OGV row.. The harmonic nature of the disturbance and the tailoring permits the analysis for the redesign to be performed on only one blade passage. Sensitivity of the pressure field upstream of the OGV's to changes in blade camber is computed, and used to modify the blade profile. The sensitivity is obtained from a linear perturbation CFD analysis; nonlinear CFD analysis and actuator disc theory (ADisc) provide validation at each step. The modifications reduce the pylon induced pressure variation at the fan by more than 70%. The presence of an interaction mechanism from the pylon to the OGV's is investigated.

Nomenclature

α	Exit Angle from OGV row
γ	Ratio of the specific heats
λ	Decay constant in ADisc analysis
Φ	Complex Potential of ADisc flow field
ρ	Density
θ	Angle
φ	Interblade phase angle
C_1	Complex Coefficient for ADisc perturbation
C_2	Complex Coefficient for ADisc perturbation
C_c	Complex Coefficient for Camber perturbation
L	Pitch of pylon
a	Speed of sound
k	Circumferential pitch of disturbance
N	Number of OGV blades in blade row
p	Pressure (Nondimensionalised by stagnation pressure)
P	Blade Pitch
u	Component of velocity along x direction
v	Component of velocity along y direction
M_x	Mach number along x direction
M_y	Mach number along y direction
$\mathcal{R}$	Real part of a complex expression
$\mathcal{I}$	Imaginary part of a complex expression

Superscripts and Subscripts

~	Perturbation quantities
0	Mean component of flow variable
d	Downstream component of flow variable in ADisc analysis
le	Leading Edge of airfoil
te	Trailing Edge of airfoil
u	Upstream component of flow variable in ADisc analysis

Introduction

It has been observed that the fan experiences high level of stresses due to excitation from the flow field (Suddhoo,

*D.Phil Student, nasng@comlab.ox.ac.uk
†Rolls-Royce Reader in CFD, giles@comlab.ox.ac.uk

Presented at the International Gas Turbine and Aeroengine Congress and Exposition
Houston, Texas - June 5-8, 1995

1992). Analysis has identified this to be due to the excitation of the fan by the pylon induced static pressure field. It has also been observed that there is a reduction of OGV efficiency, brought on by altering the incidence angle which can be attributed to the pylon induced pressure field. The jet engine of a commercial airliner is connected to the wing by the pylon which serves not only as the structural link between the wing and the engine, but also as the conduit for the generator shafts, bleed air and hydraulic and control systems. The pylon, therefore, is a large obstacle to the flow in the bypass duct and given its role, the redesign of the pylon itself is not feasible.

The presence of each component creates upstream and downstream disturbances. The OGV's also induce static pressure perturbations, but these have a very small circumferential wavelength and so decay rapidly in the axial direction and do not influence either the fan or the pylon. However, the pylon induced disturbance has a very slow decay and the pylon induced disturbance traverses the entire length of the bypass duct and interacts with the OGV's and the fan.

There have been various suggestions to prevent interaction with the pylon induced field (Suddhoo 1992) which include (a) the introduction of additional vanes to divert the flow around the pylon and (b) an increase in the distance between the OGV's and the pylon. Since the pylon induced field has a low axial decay rate, option (b) becomes unacceptable as it will require a considerable increase in engine size. Both modifications are unattractive as they will almost certainly result in increased size and weight of the engine and result in the introduction of additional components. These changes will have to be subjected to structural analysis and will be very time consuming. Therefore a passive redesign, tailoring existing components, is more appealing. Kodama and Nogano (1989) have applied actuator disc theory (Kodama 1986) to analyse the problem of stator and downstream strut interaction. Using this theory they have performed stator tailoring to suppress the pressure field of the downstream strut and have also obtained good experimental verification. Barber and Weingold (1978) have investigated the application of a Douglas-Neumann singularity method to determine the incompressible flow field through multibody cascades. Cerri and O'Brien (1989) have studied the interaction problems of a stator-strut system at the rotor trailing edge. They have successfully reduced the strut induced pressure field to the same levels of the stator induced field by redesigning the stator blades.

The current paper describes a tailoring of the OGV's, using the concept of cyclically varying camber. The resulting OGV blades will induce a pressure equal and opposite in magnitude to that induced by the pylon in the flow field upstream of the OGV's. The changes to camber will be introduced as modification to the trailing edges so that the leading edge of the blade remains unchanged. This is necessary to maintain a uniform OGV incidence angle.

The sensitivity is calculated using a linear perturbation analysis performed using the SLiQ code developed by Giles (1992). In the current study the SLiQ code is used in a 2D mode where the annulus is treated as a linear cascade with no variations in the third dimension. The harmonic nature of the disturbance and the tailoring makes it possible to evaluate just one blade passage using SLiQ. This makes the current process computationally very efficient.

Validation of the SLiQ results and predictions is carried out using two techniques. One is Actuator Disc Analysis and the other is nonlinear CFD analysis using a program called UNSFLO. Actuator Disc (ADisc) uses small perturbation theory to analyse circumferential distortions in a cascade. This theory can be used to evaluate the flow turning at the cascade to produce a required pressure field upstream of the cascade, or it can be used to determine the pressure perturbation upstream of the cascade if the downstream disturbance and the flow turning at the cascade are specified. The downstream disturbance is the static pressure variation induced by the pylon. This is calculated by executing UNSFLO on a grid with the pylon and no OGV's. This pressure variation is used as input to the SLiQ run.

The full nonlinear analysis is also performed using UNSFLO which solves the 2D Euler equations on a unstructured grid; further details are given later. The computational domain as used by UNSFLO is presented in figure 1. The X coordinate is along the axis of the engine. The Y coordinate is around the annulus. Key axial locations to note are

a. $X = -196$ is the entry to the computational domain and represents the trailing edge of the fan. This is also the entry to the SLiQ and ADisc computational domains.

b. $X = 264$ is the exit of the SLiQ and ADisc computational domain. It is also the location where the pressure variation for the pylon alone UNSFLO run is determined and used as the exit boundary condition in the SLiQ and ADisc runs.

c. $X = 2240$ is the exit of the UNSFLO computational domain.

Camber Perturbation

The camber perturbation is designed to change the exit flow angle but leave the inlet flow unaffected. The overall design goal is to eliminate all non-uniformities upstream of the OGV's in which case the leading edge geometry of all blades should be kept fixed to achieve uniform incidence Accordingly, the perturbations used in the SLiQ analysis are of the form

$$\Delta y = C_c(X - X_{le})^2 exp(-iky) \qquad (1)$$

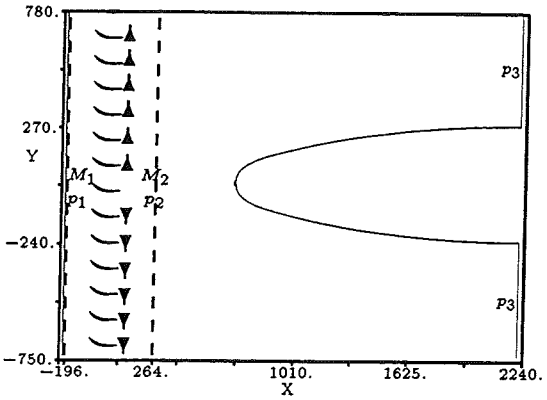

Figure 1: Pylon, OGV's and key axial locations used in analysis; arrow heads indicate direction of camber modification.

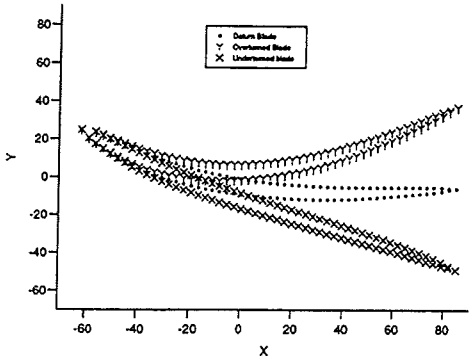

Figure 2: Camber perturbed blades.

where C_c is a complex quantity and $exp(-iky)$ represents the harmonic nature of the perturbation. The above equation translates to a exit angle variation of the form

$$\tilde{\alpha} = 2\ \cos^2(\alpha)\ C_c\ (X - X_{le})\ \exp(-iky) \qquad (2)$$

where α is the mean exit angle from the OGV row.

The sensitivity of camber to a unit perturbation is determined in the SLiQ analysis by setting $C_c = 1$. The crux of the redesign is to determine the appropriate value of C_c. Figure 2 illustrates the extreme limits of the camber perturbations for $C_c = 5 \times 10^{-2}$.

Actuator Disc Analysis

Actuator Disc analysis (ADisc) applies small perturbation theory to the analysis of circumferential distortions in a cascade. It uses a wave form solution with a prescribed circumferential variation to evaluate the transmission of disturbances through the cascade. It has been used to design rotors subjected to circumferential flow distortions by Savell and Wells (1975) and to design stators in the presence of an exit pressure distortion due to a downstream strut by Kodama and Nogano (1989). In the current work, ADisc theory is used as an alternative to the linear perturbation code to examine the differences in the solutions due to the differing modelling assumptions.

The flow on either side of the actuator disc is described by the 2D potential flow equation for an inviscid, irrotational, isentropic, compressible flow. Because of the circumferential periodicity of the pressure disturbance created by the pylon, we consider solutions of the form

$$\Phi(x, y) = \exp(\lambda x) \exp(iky) \qquad (3)$$

where $k = \frac{2\pi}{L}$, and L is the circumferential pitch of the disturbance. The two values of λ for which such solutions exist are

$$\lambda_1 = \frac{k}{1 - M_x^2}\{iM_xM_y + \sqrt{1 - M_x^2 - M_y^2}\} \qquad (4)$$

$$\lambda_2 = \frac{k}{1 - M_x^2}\{iM_xM_y - \sqrt{1 - M_x^2 - M_y^2}\} \qquad (5)$$

where M_x and M_y refer to Mach numbers in the x and y directions respectively. Since the real part of λ_1 is positive, the corresponding flow solution has an exponential increase in the axial direction, whereas the real part of λ_2 is negative and so its corresponding flow solution has an exponential decrease in the axial direction.

A general flow solution with the required circumferential periodicity is a sum of an arbitrary multiple of each of these two flow solutions. Perturbations in the pressure, density and velocity components can be related to the potential solution to obtain the following expressions, in which C_1 and C_2 are complex constants giving the arbitrary amplitudes of the two component modes.

$$\frac{\tilde{p}}{p_0} = \{C_1 exp(\lambda_1 x) + C_2 exp(\lambda_2 x)\} \exp(iky) \qquad (6)$$

$$\frac{\tilde{\rho}}{\rho_0} = \frac{1}{\gamma}\{C_1 exp(\lambda_1 x) + C_2 exp(\lambda_2 x)\} \exp(iky) \qquad (7)$$

$$\frac{\tilde{u}}{a_0} = -\left\{\frac{\frac{\lambda_1}{k}}{M_x\left(\frac{\lambda_1}{k}\right) + iM_y} C_1 \exp(\lambda_1 x) + \frac{\frac{\lambda_2}{k}}{M_x\left(\frac{\lambda_2}{k}\right) + iM_y} C_2 \exp(\lambda_2 x)\right\} \frac{\exp(iky)}{\gamma} \qquad (8)$$

$$\frac{\tilde{v}}{a_0} = -\left\{\frac{i}{M_x\left(\frac{\lambda_1}{k}\right) + iM_y} C_1 \exp(\lambda_1 x) + \frac{i}{M_x\left(\frac{\lambda_2}{k}\right) + iM_y} C_2 \exp(\lambda_2 x)\right\} \frac{\exp(iky)}{\gamma} \qquad (9)$$

The actual physical perturbation is always the real part of the complex quantity given in these equations. The complex representation can be viewed here as simply a convenience to simplify the construction of the general solution. It is however a fundamental aspect of the linear perturbation code, SLiQ. To understand this it is helpful at this point to note that one feature of the complex solution to the potential flow equation, and the associated perturbation flow variables is that

$$U(x, y + \Delta y) = e^{i\phi} U(x, y), \quad \phi = k\,\Delta y \qquad (10)$$

Here, U can be viewed either as the complex potential Φ, or as the vector of perturbed quantities $(\tilde{p}, \tilde{\rho}, \tilde{u}, \tilde{v})$. Because of this periodicity feature, the same flow solution would have been obtained if the perturbation equations of motion were solved on the strip $0 \leq y \leq \Delta y$ with the periodic boundary condition

$$U(x, \Delta y) = e^{i\phi} U(x, 0), \quad \phi = k\,\Delta y \qquad (11)$$

This, in essence, is how the linear perturbation code SLiQ operates.

In the ADisc analysis, the flow on either side of the disc has the above form (with the same values for the stagnation quantities assuming no loss in the actuator disc), but with constants C_{1u}, C_{2u} upstream of the disc and constants C_{1d}, C_{2d} downstream of the disc. Four equations or conditions are now required to determine these constants.

In the analysis mode, determining the flow field generated by the interaction of the pylon and OGV's. C_{1d} is determined by the pressure disturbance created by the pylon alone. C_{2d} is obtained by specifying the flow angle at the exit of the actuator disc (equal to the blade trailing edge metal angle α). Since $v = u\tan(\alpha)$, the corresponding perturbation equation is

$$\tilde{v} = \tan(\alpha)\tilde{u} \qquad (12)$$

and substitution of the downstream expressions for $\tilde{v}, \tilde{u}$ gives the algebraic relation between C_{1d} and C_{2d}. C_{2u} is set to zero since the flow should approach a uniform state far upstream of the disc. C_{1u} is determined by the final condition, the matching of mass flow across the disc.

$$(\tilde{\rho}u + \tilde{u}\rho)_u = (\tilde{\rho}u + \tilde{u}\rho)_d \qquad (13)$$

Substituting the equations for the perturbation quantities gives C_{1u} as a function of C_{1d} and C_{2d}.

In the design mode, the objective is to determine a cyclic variation in the OGV trailing edge angle such that there is no flow disturbance upstream of the actuator disc. In this case, C_{1u} and C_{2u} are both set to zero. C_{1d} is again determined by the pylon pressure field in the absence of the OGV's, and C_{2d} then comes from the condition of matching the mass flow across the disc. The perturbation in exit angle comes from perturbing the equation $v = u\tan(\alpha)$ to obtain

$$\tilde{v} = \tan(\alpha)\,\tilde{u} + u\sec^2(\alpha)\,\tilde{\alpha} \qquad (14)$$

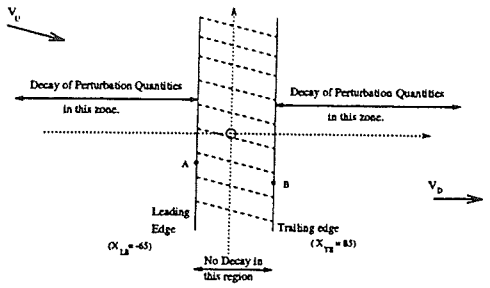

Figure 3: Thick Actuator Disc

Given the flow perturbations based on C_{1d} and C_{2d}, this equation defines the exit angle perturbation $\tilde{\alpha}$ to be a complex quantity of the form

$$\tilde{\alpha}(y) = C_\alpha e^{iky} \qquad (15)$$

If the n^{th} OGV trailing edge is at $y = y_n$, then the actual physical perturbation angle would then be

$$\tilde{\alpha}_n = \mathcal{R}\left(C_\alpha e^{iky_n}\right) \qquad (16)$$

Thick Actuator Disc Theory

The use of the equations derived in the preceding section yields a discrepancy between the pressure predicted by ADisc and that calculated using SLiQ and UNSFLO. ADisc always under predicts the perturbation quantities. Investigation revealed that this discrepancy is related to the absence of any consideration for the width of the OGV row. This results in the ADisc model predicting a larger decay of the perturbation variables. To circumvent this the thick actuator disc formulation was created.

In this model the axial coordinates of the leading and trailing edge of the OGV are taken into account, as well as its mean stagger. The potential flow representation of the flow field remains valid upstream and downstream of the OGV's as indicated in Figure 3. The exit flow angle condition is applied at the trailing edge plane to determine the relationship between C_{1d} and C_{2d} The condition of matching mass flow is applied to link the flow states at corresponding points A and B in the leading and trailing edge planes offset because of the mean stagger of the OGV's. No model is necessary for the flow within the OGV passages.

The modified thick actuator disc equations are implemented in a computer program which requires as input

a. the magnitude of the pylon induced pressure perturbation (at $x = 264$)

b. the variation of trailing edge angle of the OGV's.

The constants C_{1u}, C_{1d} and C_{2d} are computed and the pressure is plotted for any required x coordinate. When used in the inverse mode with the pylon induced pressure field at $x = 264$ the program calculates the necessary variation in the flow exit angle from the OGV's to achieve total suppression of the disturbance upstream of the OGV's. These results are used as comparisons in the runs described in the following sections. In all subsequent sections the term ADisc will refer to the thick actuator disc analysis.

Linear Perturbation Analysis

The current work is aimed at redesign using sensitivities computed by a linear perturbation code. The code used was SLiQ, developed by Giles (1992) at MIT. SLiQ is an acronym for Steady/Linear/Quadratic, which refers to the first three terms of the asymptotic expansion that are computed in this method. In this code the unsteady, three dimensional Euler's equations are solved on a structured grid. The unsteady solution is assumed to have an asymptotic form. The first term of this expansion represents the nonlinear steady-state base flow. The second term is the linear perturbation to the base flow, in unsteady computations it has a zero time average, but in this work it gives the linear sensitivity of the steady flow to grid perturbations due to design changes. The third term, the quadratic term, reveals the change to the mean flow due to the time averaged effect of unsteadiness; it is not used in the current work.

In the work in this paper, SLiQ is executed in a 2D mode where the OGV row is modelled as a linear cascade. It is assumed that there is no variation in either the geometry or the flow in the third dimension. When performing a linear perturbation analysis for unsteady motion in such cases, the flow solution is expressed as being the real part of a complex quantity of the form

$$\tilde{U}(x,y)\exp(i\omega t).$$

It is well-known that in linear unsteady analysis, the general solution can be decomposed into a sum of particular solutions satisfying the periodicity condition

$$\tilde{U}(x,y+P) = e^{i\phi}\tilde{U}(x,y), \tag{17}$$

where ϕ is known as the inter-blade phase angle and P is the blade pitch. The use of this equation as a periodic boundary condition allows the computation to be performed on a single blade passage, and then the solution in other passages can be reconstructed from

$$\tilde{U}(x,y+nP) = e^{in\phi}\tilde{U}(x,y). \tag{18}$$

As indicated in the discussion of the actuator disc analysis, exactly the same approach is used by SLiQ for the analysis of the steady perturbation due to the cyclic disturbance of the pylon's pressure field or a cyclic variation in the OGV camber. The inter-blade phase angle is given by

$$\phi = kP = \frac{2\pi P}{L} = \frac{2\pi}{N} \tag{19}$$

where N is the number of OGV's per pylon in the 2D cascade. In the current SLiQ analysis for an annular cascade with one pylon, N is the number of OGV's in the cascade.

In the analysis mode, the perturbation pressure field due to the pylon is specified through the downstream boundary conditions. The discrete linear equations for the interior of the domain come from a natural linearisation of the nonlinear discrete equations coming from a standard finite volume discretisation. This includes the linearisation of the solid wall boundary conditions on the OGV's. The inter-blade phase angle is specified, the complex flow solution is computed for the single passage, and then the real perturbation quantities can be reconstructed for any blade passage in a post-processing step.

In the design mode, the perturbation in the camber of the OGV's defines a consistent linear perturbation of the body-fitted computational grid. This introduces a source term into the discrete linear equations throughout the grid. Because the camber perturbation has cyclic periodicity, it is again possible to perform the calculation on a single blade passage by imposing the complex periodic boundary condition with the appropriate inter-blade phase angle. The design mode is executed without the downstream boundary condition imposing the pressure perturbation of the pylon. Instead, the goal is to determine the camber perturbation which generates an upstream flow perturbation equal in magnitude and opposite in sign to that produced by the pylon's interaction with the OGV's. Then, by linearity, the sum of the two solutions will give a combined flow solution corresponds to the presence of the pylon and the cyclically cambered OGV's and giving no flow perturbation upstream of the OGV's, (except for the very local pressure field associated with each OGV).

Non-linear Analysis

As a verification tool a nonlinear analysis code "UNSFLO" was used. UNSFLO can solve for steady or unsteady, viscous or inviscid equations of motion in two dimensions. It can handle various kinds of unsteadiness and arbitrary wake/rotor, stator/rotor pitch ratios. It uses highly accurate non-reflecting boundary conditions developed by Giles (1988), which reduce the non-physical reflections at inflow and outflow boundaries. The computations are performed on an unstructured triangular grid, generated by an advancing front grid generator developed by Lindquist and Giles (1990).

The use of UNSFLO for pylon/OGV interactions has been validated by Suddhoo using experimental data (Suddhoo 1992). In the current application, UNSFLO is used in

its inviscid mode, which uses the Lax-Wendroff algorithm to solve the Euler equations (Giles and Haimes 1993). Though there are viscous effects present in the flow in the vicinity of the OGV's, the pressure disturbance is an inviscid feature, thereby permitting the use of UNSFLO and SLiQ in the inviscid mode.

Comparability of Various Solutions

In studies where there is a comparison of data from various sources, it is necessary to ensure that the results being compared are obtained from computations on the same flow conditions. This can be done by identifying a parameter of the flow which is common to all the calculations and to ensure that this variable is maintained constant. The location of the parameter was chosen to be at $x = 264$ (shown in figure 1) because this location was common to all computations (SLiQ, UNSFLO and ADisc). Mach number was selected as the key parameter since it is critical in determining the decay rate λ. As indicated by figure 1, location 1 refers to the inlet $X = -196$, 2 refers to $X = 264$ (exit of SLiQ and ADisc) and 3 refers to the exit of the UNSFLO flow domain. The correct M_2 (Mach number at Location 2) in the UNSFLO calculations was obtained by altering the exit pressure p_3. In the following runs M_2 was maintained at about 0.38.

Redesign of OGV's

It can be demonstrated from actuator disc theory that the pressure distribution is very sensitive to a change in the angle of the flow leaving the trailing edge of the OGV's. This sensitivity was used in the stator tailoring exercise. In all the plots included here the results from UNSFLO are duplicated so they appear as though two pylons and twice as many blades were present. The steps in the redesign include:

i. Evaluation of the initial geometry to determine the pressure disturbance that propagates upstream of the OGV's. This analysis was performed using UNSFLO. The computational domain included the OGV's and the pylon. The analysis was performed for $p_3 = 0.7$ (see the previous section for details on p_{1-3}), and M_1, M_2 were determined. To ensure that the following runs were comparable, the desired M_2 was closely replicated by altering the exit pressure boundary condition as required. A circumferential line plot of pressure obtained at the entrance to the computational domain is presented in figure 4.

ii. Determination of the pressure field of the pylon alone. This analysis is used to determine the pylon induced pressure field, so the calculation is carried out on a grid where the blades are absent. The pressure variation that is obtained at $x = 264$ is the pressure perturbation that is the input to the SLiQ run and the ADisc run. To ensure comparability with the previous run, p_3 is again adjusted in such a way that M_2 is the same as before. The line plot of p_2, the pressure measured at $x = 264$ is presented in figure 5.

iii. A validation of SLiQ is carried out by analysing the unmodified blades under the influence of the pylon-alone pressure field determined in the previous step. The grid used by SLiQ is presented in figure 6. The solution obtained for the single blade passage defines the solution for the whole annulus using equation (18). The pressure variation predicted by SLiQ, UNSFLO and ADisc at the entry to the computational domain is shown in figure 7. The comparison is excellent. This validates the assumption that the influence of the pylon can be isolated and the redesign carried out on the OGV's alone; ie. the interaction is linear. It

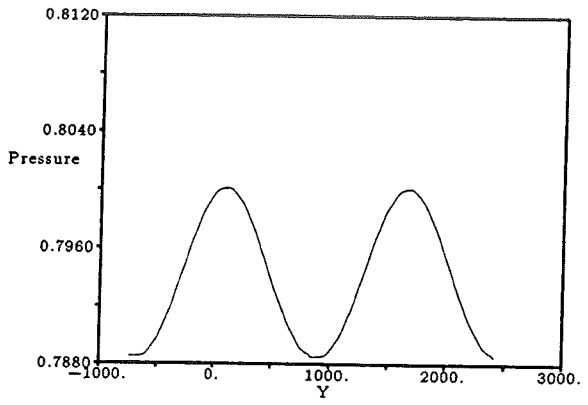

Figure 4: Circumferential Line plot of pressure at entry to computational domain at $x = -196$

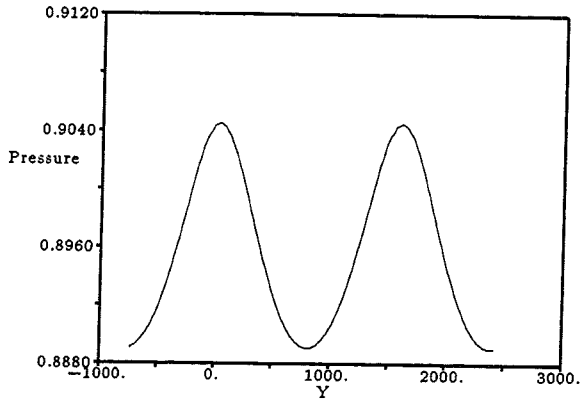

Figure 5: Line plot of pressure from UNSFLO measured at $x = 264$ which represents the exit boundary in SLiQ analysis.

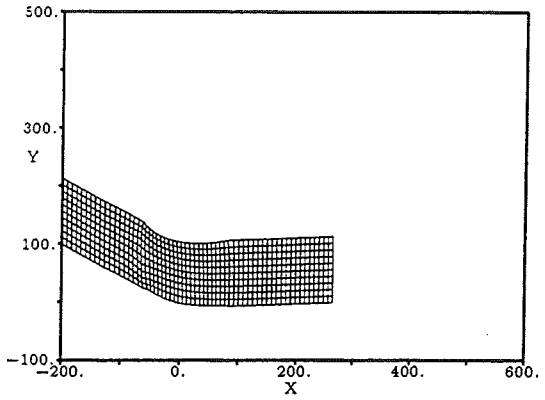

Figure 6: SLiQ computational Grid for uniform OGV's.

also validates the previous step and confirms the possibility of using SLiQ in conjunction with UNSFLO.

iv. The success of the previous step confirms the assumption that the problem can be viewed by isolating the OGV's from the pylon. The next step is to determine the sensitivity of pressure to change in camber. SLiQ is used to calculate the linearised effect of a circumferential variation in camber of unit magnitude. Again the calculation is performed using one OGV passage and then the variation in other passages is reconstructed using equation (18). The circumferential pressure perturbation upstream of the OGV's is shown in figure 8.

v. Using the sensitivity calculated in the previous step, the required change in camber of the OGV blades is determined. This is expressed as a harmonically varying change. The change when applied to the blades, serves to divert the flow around the pylon and therefore reduce the build up of static pressure in front of the pylon. In figure 1 the arrows at the trailing edges of the OGV's indicate the direction of suggested changes.

vi. For initial verification a computational domain involving just the redesigned blade row is analysed by UNSFLO. The upstream pressure is compared to the pressure measured at the same location in the uniform OGV configuration. They are required to be equal and opposite. The pressures predicted by UNSFLO, SLiQ and ADisc are presented in figure 9.

vii. As the final step, the predicted blade geometry is inserted into the OGV pylon grid and analysed with UNSFLO. This should confirm a complete suppression of the flow upstream of the OGV's. However, the result (plotted in figure 10) shows a residual pressure variation. When viewed with the pressure variation of the datum OGV row, it becomes evident that the correction prescribed has "overcorrected" the error.

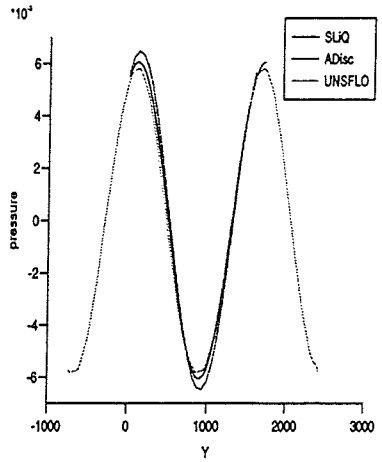

Figure 7: Comparison of circumferential pressure variation predicted by SLiQ, UNSFLO and ADisc upstream of OGV's at $x = -196$.

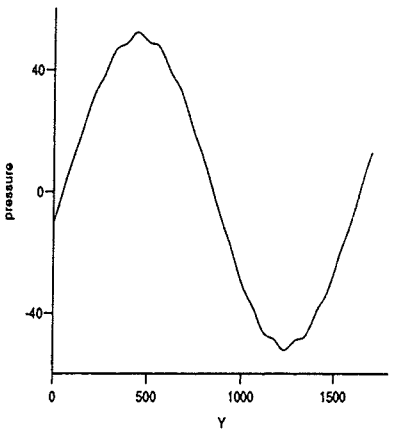

Figure 8: Line plot of pressure at inlet to computational domain, at $x = -196$, for a unit perturbation in camber, calculated by SLiQ.

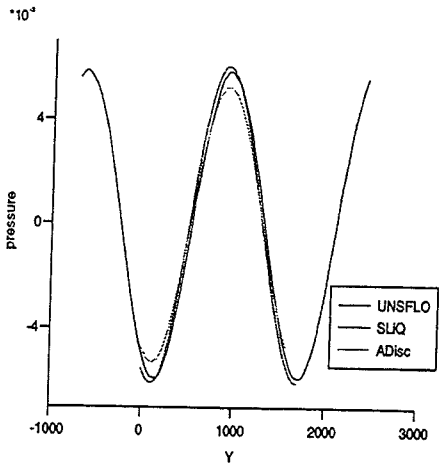

Figure 9: Comparison of pressure variation predicted upstream of a cascade of tailored blades, at $x = -196$.

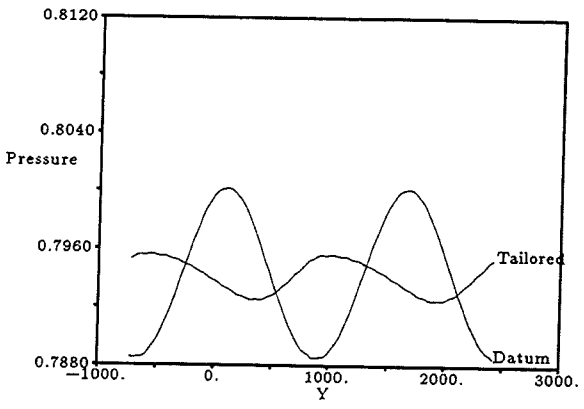

Figure 10: Comparison of pressure variations upstream of the OGV row at, $x = -196$, for a OGV-pylon configuration using uniform and tailored blades.

An Interaction Effect

The reason for the over-correction of the re-designed OGV's was investigated by using UNSFLO to perform a number of nonlinear OGV/pylon calculations. The circumferential pressure variation upstream of the OGV's is plotted in figure 11. Each of the three curves represents the difference in pressures obtained from two nonlinear calculations, one using the re-designed OGV's and the other using the original OGV's. The two grids are very similar and the calculations were performed for the same Mach number M_2 as discussed earlier, so the pressure difference corresponds solely to the change in the flow field due to the change in the OGV's. The factor that is different for the three curves is the pylon downstream of the OGV's. One curve corresponds to calculations using no pylon, just the OGV's. A second curve corresponds to calculations using the regular (thick) pylon. The third curve uses a thin pylon of half the thickness of the regular pylon.

The results show that the pressure perturbation due to recambering the OGV's is greater in the presence of the thick pylon than with the thin pylon or no pylon at all. The linear SLiQ analysis corresponds to a linearisation of the nonlinear calculation without the downstream pylon. Using the SLiQ analysis to design the recambering produces modified OGV's which, in the presence of the thick pylon, will then produce too large a pressure change, over-correcting the original pressure disturbance due to the pylon. The results in figure 11 are therefore consistent with the observed over-correction.

The cause of the results in figure 11 is less clear. There are two possible explanations. The first is a feedback phenomenon. The change in the OGV camber produces flow field changes downstream of the OGV as well as upstream. In the absence of a downstream pylon, the downstream changes are irrelevant, but when there is a pylon it may cause a 'reflection' of the disturbance producing a new, although much smaller, pressure perturbation which will affect the OGV's. The magnitude of the reflection will depend on the thickness of the pylon, because it can be shown mathematically that in the limit in which the pylon becomes a flat plate there is no reflection.

The second possibility is nonlinear effects. The whole basis of the linear approach using SLiQ is that the separate pressure perturbations due to the pylon and the recambering of the OGV's can be linearly superimposed. In practice, this is not strictly correct since the equations are nonlinear. The magnitude of the error will be proportional to the product of the two perturbations, and so will be roughly proportional to the thickness of the pylon.

Despite the over-correction the design approach has been successful in greatly reducing the pressure variation upstream of the OGV's. If even more reduction is needed, the next step would be to use the results of the nonlinear anal-

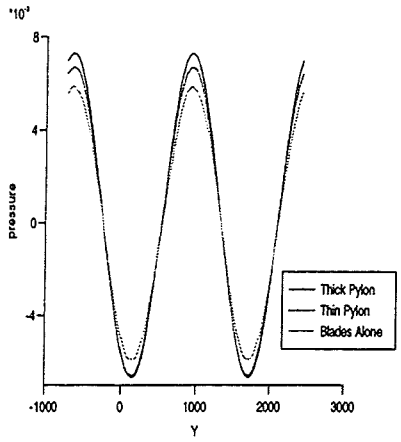

Figure 11: Influence of pylon size on upstream pressure changes due to recambering

ysis giving the remaining pressure variation; feeding these into a further iteration of the design process would give an additional much smaller camber perturbation to eliminate the majority of the remaining pressure perturbation.

Applicability to the Design Process

One problem with this design procedure is that it generates a set of OGV's each of which is unique. This leads to unacceptable additional costs both in the manufacture of the OGV's and in the airlines' costs of maintaining stocks of spare parts. A practical compromise is to use a limited number of different OGV's; for example three, one with the datum exit flow angle, one with overturning and one with underturning. These can then be grouped and collectively designed to completely cancel the first circumferential harmonic of the pressure field generated by the pylon. The design can still be performed using the linear tools described in this paper. The OGV trailing edge flow angle is now a square wave function, corresponding to the different groups of blades. This square wave can be decomposed into a sum of circumferential harmonics, each of which can be analysed separately with its own steady interblade phase angle. By linear superposition the results can then be combined to give the overall perturbation flow field. Linear scaling of the geometric perturbation will then lead to cancellation of the first harmonic of the upstream pressure perturbation. Additional harmonics can also be eliminated using a larger number of different blades. However, this may be unnecessary since these higher harmonics decay axially at a faster rate and so are less likely to adversely affect the fan.

Conclusions

The use of a linear perturbation code to determine sensitivities and redesign and OGV row is demonstrated. The redesign was successful in that it achieved more than 70% reduction in the static pressure variation that was exciting the fan. A feedback coupling between the pylon and OGV's was identified as the reason that even better reduction was not obtained.

Acknowledgments

The authors are grateful to Rolls-Royce plc for their financial support, and Drs P. Stow, A. Suddhoo and A. Parry for their technical collaboration in the development of the computational model.

References

Barber, T. J. and Weingold, H. D., 1978, Vibratory Forcing Functions Produced by Nonuniform Cascades. *ASME Journal of Turbomachinery*, 100(77-GT-57):82–88, January 1978.

Cerri, G. and O'Brien, W. F., 1989, Sensitivity Analysis and Optimum Design Method for Reduced Rotor-Stator-Strut Flow Interaction. *ASME Journal of Turbomachinery*, 111(88-GT-310):401–408.

Giles, M. B. and Haimes, R., 1993, Validation of a Numerical Method for Unsteady Flow Calculations. *ASME Journal of Turbomachinery*, 115(91-GT-271):110–117.

Giles, M. B., 1988, Non-Reflecting boundary conditions for Euler equations. Technical Report TR-88-1, MIT Computational Fluid Dynamics Laboratory.

Giles, M. B., 1992, An Approach for Multi-Stage Calculations Incorporating Unsteadiness. ASME paper 92-GT-282 presented at the International Gas Turbine and Aeroengine Congress and Exposition, Cologne, Germany.

Kodama, H. and Nogano, S., 1989 Potential Pressure Field by Stator/Downstream Strut Interaction. *ASME Journal of Turbomachinery*, 111(88-GT-54):197–203.

Kodama, H., 1986, Performance of Axial Compressor With Nonuniform Exit Static Pressure. *ASME Journal of Turbomachinery*, 108(85-IGT-43):76–81.

Lindquist, D. R. and Giles, M. B., 1990, Generation and use of unstructured grids for turbomachinery. Proceedings of Computational Fluid Dynamics Symposium on Aeropropulsion, NASA CP-10045.

Savell, C. T. and Wells, W. R., 1975 Rotor Design to Attenuate Flow Distortion: Part 1 – A Semiactuator Disc Analysis. *ASME Journal of Engineering for Power*, 97.

Suddhoo, A., 1992 Pylon/OGV/Fan Interaction in the TRENT 600 & 700. Technical Report TSG0622, Theoretical Science Group, Rolls-Royce plc.